Tracking Excited State Dynamics with Coherent Control: Automated Limiting of Population Transfer in LDS750

Omer Nahmias, Oshrat Bismuth, Ofir Shoshana, and Sanford Ruhman*

Department of Physical Chemistry and the Farkas Center for Light Induced Processes, The Hebrew University, Jerusalem 91904, Israel

Received: May 4, 2005; In Final Form: July 24, 2005

Closed loop automated pulse shaping experiments are conducted to investigate population transfer in solutions of the laser dye LDS750 in acetonitrile and ethanol. Guided by a genetic algorithm, the optical phases of broadband noncollinear parametric amplifier pulses are modulated by a micromachined deformable mirror to minimize sample fluorescence. The objectives were to test if nonlinearly chirped pulses could reduce population transfer below levels attained by their linearly chirped analogues, and if so, whether the resulting pulse shapes could be rationalized in terms of the photoinduced molecular dynamics. We further aimed to discover how the optimal solutions depend on the pulse fluence, and on the nature of the solvent. Using frequency resolved optical gating, the optimal field is shown to consist of a transform limited blue portion, which promotes population to the excited state, and a negatively chirped red tail, which follows the Stokes shifting of the excited density and dumps it back down to the ground state through stimulated emission. This is verified by comparing the optimal group delay dispersion with multichannel transient absorption data collected in acetonitrile. The optimal pulse shape was not significantly affected by variation of pulse fluence or by the change of solvent for the two polar liquids investigated. These results are discussed in terms of accumulated insights concerning the photophysics of LDS750 and the capabilities of our learning feedback scheme for quantum control.

Introduction

Shaping ultrashort laser pulses to control photoinduced molecular dynamics is the subject of active current investigation.[1−5] Starting more than a decade ago, theoretical studies demonstrated that properly chirped broad-band pulses could improve on the performance of their transform limited analogues in achieving a variety of dynamic goals, involving both the excited and ground electronic surfaces.[6−9] Considering resonant excitation of a one-dimensional photodissociative model, Ruhman and Kosloff showed that with the right amount of negative linear chirp, a single excitation pulse comprises a complete pump and dump sequence.[10] The leading blue edge of the spectrum promotes density on to the reactive excited state, with the trailing lower frequency field components following the evolving population, and dumping it back down onto the ground state. In that study, the focus was on generating large amplitude ground state vibrational coherences. Since the excited population evolves for a significant period of time on the dissociative potential before being dumped back to the ground state, large displacements from the equilibrium internuclear distance were achieved, involving high vibrational levels in the re-formed ground state population. Conversely, the same linear chirp had the effect of minimizing the net transfer of population to the excited state, effectively inducing transparency.

In a series of pioneering experiments, Shank and co-workers produced ultrafast pulses with sufficiently broad band coherent spectra for testing these predictions on real molecular systems.[11] Cerullo et al. investigated the effect of linear chirp on the emission of LD690 and LDS750 dye solutions using pulses which were 12 fs in duration. At negligible excitation fluences, the chirp had no effect on the fluorescence signal. As the fluence was increased, fluorescence intensity was minimized by a pulse group velocity dispersion (GVD) of nearly (−120 fs^2/rad) for both dye solutions, indicating that at this particular chirp rate the ultimate population transfer to the excited state was lowest in both cases. The optimal chirp for obtaining this minimum was found to be independent of the pulse fluence. Varying the chirp rate in either direction increased the emission intensity in both dye solutions studied, although the details of the variation of fluorescence intensity with changes in group delay dispersion (GDD) at a given fluence differed from dye to dye.

Model calculations in terms of two bound electronic states and one low frequency displaced nuclear coordinate qualitatively captured the observed behavior, without explicit representation of solvent dissipation. The single 170 cm^{-1} harmonic mode used in the model was purported to schematically represent the effects of both intramolecular and intermolecular coordinates on the rapid dynamic Stokes shifting of the dye emission. Despite the qualitative agreement of the model with the experimental results, the underlying physics is very different. In the model, nuclear motion in the form of a coherent wave packet along a single displaced or dissociative mode causes a rapid continuous variation of the instantaneous emission spectrum. The pulse chirp must compensate for this rapid variation if effective stimulated emission is to be achieved by the trailing edge of the excitation field. In contrast, in the large polyatomic laser dyes studied, a multitude of intramolecular active modes as well as solvent motions cause irreversible dynamic Stokes shifting of the fluorescence. Following this process, and especially separating out the solvation relaxation and breaking it up into inertial and relaxational components, has been a major focus

* To whom correspondence should be directed. E-mail sandy@fh.huji.ac.il.

10.1021/jp052313s CCC: $30.25
Published on Web 08/27/2005

of interest for ultrafast spectroscopists and theorists alike.[12−18] None the less, no comparative experiments concerning the effect of linear chirp on the transfer of population were conducted with the same dye in different solvents in order to check the involvement of fast solvation in determining the optimal chirp. Finally, using similar laser pulses Bardeen et al. investigated the influence of linear chirp on the aspects of resonant electronic excitation addressed by Ruhman and Kosloff,[10] i.e., on the generation of ground-state vibrational wave packets.[19] As predicted earlier, the right amount of negative chirping did not deteriorate, and in some cases even enhanced the generation of compact ground-state vibrational coherences via resonant impulsive Raman scattering (RISRS) both in dye solutions and in suspensions of the bacteriorhodopsin protein, as attested to by the periodic spectral modulations they induced in pump−probe signals. This effect has subsequently been used as a diagnostic for identifying spectral modulations due to RISRS-induced coherences.[20]

Theoretical simulations, including those cited above, clearly demonstrate that *nonlinearly* chirped pulses can do even better at attaining a variety of dynamic control objectives in molecular chromophores. The introduction of automated pulse shaping devices and learning computer algorithms to guide them, have made it possible to seek out such optimally shaped pulses in a straightforward and systematic fashion. Using feedback coherent control, Bardeen et al.[21] investigated the efficiency of various shaped titanium sapphire laser pulses in transferring population to the excited state of IR125 dye molecules in solution, again by following the fluorescence yields. The acousto-optic shaper used was programmed to vary the pulse spectrum by selective attenuation and to introduce various amounts of linear chirp only. While the earlier study demonstrated that *minimum* population transfer was an objective with a well-defined optimal solution in terms of linear chirp, the automated control experiment conducted was aimed at finding a pulse which *maximized* fluorescence. This choice, and the limitation of the chirp to GVD alone, produced somewhat trivial optimal solutions which could be explained in terms of the linear absorption spectrum of IR125 etc.

In the experiments reported here, an automated pulse shaper based on a micromachined deformable mirror (DM) and guided by a genetic algorithm were used in conjunction with a broadband noncollinear optical parametric amplifier (NOPA), to investigate population transfer in LDS750 dye solutions in acetonitrile and in ethanol. Our choice of returning to a laser dye solution as a test case stems primarily from the convenient presence of a built in gauge for residual excited-state population in the form of spontaneous emission. In the case of this particular dye, a large body of work concerning ultrafast photophysics exists which can be used to compare with the results of our study.[22−24] Contrary to the assertion of Cerullo et al. that solvent relaxation contributes significantly to dynamic Stokes shifting of LDS750, much of the excited state dynamics recorded in those studies were dominated by intramolecular coordinates, with the steady state emission taking place from an isomer of the optically accessed excited state (see Figure 1 for absorption and spontaneous emission curves). LDS750, like other styryl dyes, is large and flexible enough to conceptually constitute its own "bath". None the less substantial discrepancies between the various studies cited make its renewed investigation with this novel spectroscopic tool intriguing.

Our main objective here is to discover whether nonlinearly chirped pulses made available by flexible pulse-shaping methods can reduce population transfer in a polyatomic chromophore in solution below levels attained by linear chirp alone, and if so, whether the resulting pulse shapes can be rationalized in terms of the underlying photoinduced molecular dynamics. We further aim to test whether the optimal pulse shape for minimal population transfer is a function of the pulse fluence or of the solvent. The latter is investigated to determine whether rapid inertial stages of solvation contribute significantly to the early stages of this dye's emission Stokes shifting.[25]

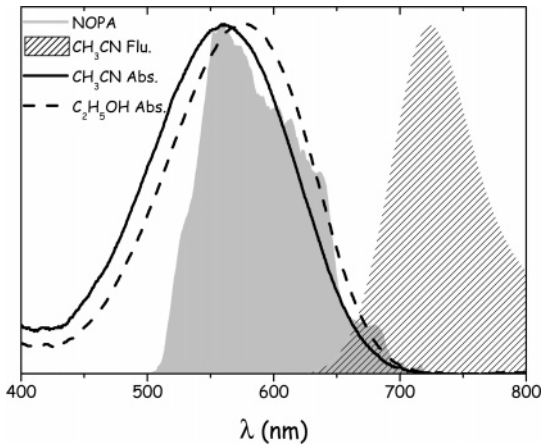

Figure 1. NOPA pulse intensity spectrum along with LDS750 absorption curves in acetonitrile and in ethanol. A fluorescence spectrum of LDS750 in acetonitrile adapted from ref 22 is depicted as well.

Results show that the optimal fields are intricately and nonlinearly chirped. Comparison with multichannel transient absorption data collected in the same solutions demonstrates that the pulse chirp reflects the spectral evolution of an impulsively excited sample, involving the ground state bleach, excited state absorption, and emission. The optimal group delay dispersion was not significantly effected by variation of pulse fluence or by the change of solvent for the two polar liquids investigated. These results will be discussed in terms of accumulated insights concerning the photophysics of LDS750 and the capabilities of learning feedback schemes for quantum control.

Experimental Section

The laser system used for quantum control was a home-built multipass amplified titanium sapphire oscillator, operated at a repetition rate of 1 kHz.[26] Its output consisted of 30 fs pulses with spectra peaked at 790 nm, and containing ∼0.5 mJ of energy. Here, 50% of the amplifier output pumped a commercial NOPA plus (Clark-MXR), which was reconfigured to a single pass of amplification in 2 mm of BBO.[27] The NOPA output pulses contained 5 μJ of energy, with a spectrum of ∼100 nm fwhm centered at 600 nm which are precompressed in a BK7 prism pair with an apex to apex distance of 550 mm (See Figure 1 for a typical pulse spectrum). These pulses are passed into a zero dispersion shaper constructed from a 300 l/mm grating, a silver coated 500 mm focal length spherical reflector, and a 19 channel gold coated DM (OKO Flexible Optical) positioned at the Fourier plane.[28] The DM and the grating are vertically and not horizontally displaced to reduce the intrinsic dispersion of the pulse shaper. While this shaper was capable of completely compressing the NOPA pulses, the precompensation in a prism pair was required for extending its range to allow the generation of the negatively chirped pulses needed in the present application.[29]

The beam intensity is adjusted to ∼100 nJ by reflection off an aluminum coated linear variable beam splitter (Reynard) and

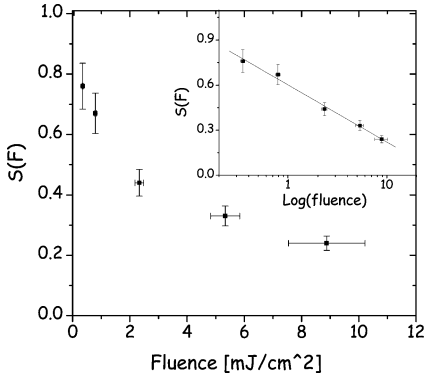

Figure 2. Normalized degree of fluorescence saturation for optimally shaped pulses ($S(F)$) plotted as a function of the pulse fluence in acetonitrile solutions.

directed into the sample using a post polished 45° off-axes paraboloid ($f = 100$ mm) which focuses the beam to a diameter of ~40μm. LDS750 dye (Aldrich), Acetonitrile (analytical reagent) and Ethanol (absolute), were used as received from the manufacturer. The solutions were pumped through a 200 μm flow cell equipped with 150μm quartz windows at a rate which replenished the sample between pulses. The peak optical density of the acetonitrile solutions used in the control experiments was ~0.3, leading to an attenuation of the excitation beam by no more than 25%. The optical density of the ethanol solutions was even lower, absorbing less than 10% of the pulse energy. Fluorescence from the dye cell was collected with an $f = 1$ lens at an angle of ~30° from the excitation beam, and detected by an amplified silicon photodiode through an 695 nm high pass cutoff filter to discriminate fluorescence from pump pulse scatter. The sample cell, fluorescence collection optics, and detector were all mounted on a translation stage, allowing the sample to be continuously displaced from the beam focus without affecting the fluorescence collection efficiency. The cell displacement was used to control the excitation fluence by varying the beam diameter while conserving the excitation pulse energy.

Fluorescence minimization runs were conducted at fluences which are limited above by supercontinuum generation, and below by the absence of substantial fluorescence saturation, with the resulting range spanning a factor of 25 as detailed in Figure 2. The beam diameter at the various cell displacements was determined by measuring transmission through a 50 μm pinhole and assuming a Gaussian intensity distribution. The fluorescence signal from the photodiode, V_f, is digitized and used as feedback in a genetic algorithm which minimizes the fluorescence signal by defining $-V_f$ as the pulse fitness. The algorithm used has been described in the literature and is based on random mutations.[30] The total population of a given generation consisted of 45 solutions for voltages on the mirror, 5 of which were parents or best solutions from a previous generation, and 40 offspring generated by their mutation. The optimization run was terminated when no further improvement in the fitness was obtained for at least 5 generations within the experimental noise (~1%). The changes in the optimal mirror voltages from the previous generation was another convergence criterion, and was required to be below 5 V on all pixels before the termination of an optimization run.

After minimization was completed the optimal pulse was characterized in a polarization gate FROG setup which uses a 0.5 mm fused silica flat as the Kerr medium.[31] A fraction of the remaining amplifier fundamental at 790 nm was used for the Kerr pump, providing a gating half-width of ~25 fs. The

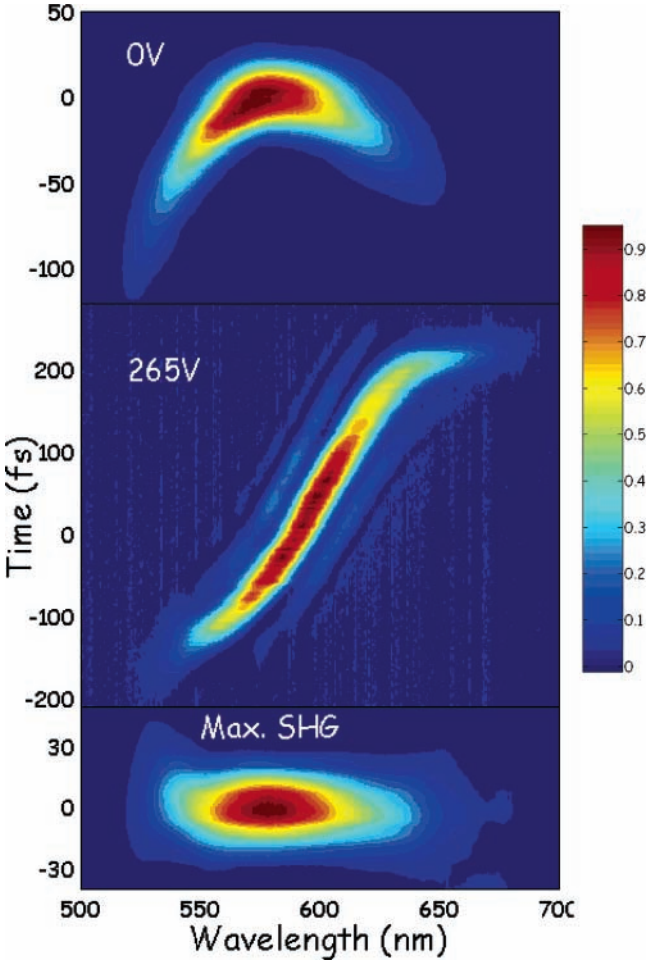

Figure 3. Polarization gate FROG traces of shaped NOPA pulses. The upper panel depicts a contour plot of the FROG data with zero voltage on all mirror channels. The middle panel shows the same plot with maximum voltage on all pixels, and the bottom panel shows that for a pulse which has been compressed by maximizing SHG in a 20 μm BBO crystal. Notice the differences in Kerr gate delay scales for the different panels.

gate/NOPA time delay was automatically varied and the gated radiation directed by fiber to a $^1/_8$ m imaging spectrograph (Oriel) equipped with a CCD camera (Andor technology). FROG contour plots of the NOPA pulses with zero and with the maximum 265 V on all DM channels are presented in Figure 3, along with one obtained with optimally compressed pulses using second harmonic generation (SHG) maximization in a 20 μm BBO crystal.

To verify that the optimal solutions obtained were not limited by the range of deformation provided by the DM, we checked that none of the 19 mirror voltages was either saturated or set to zero when the routine converged. As another test, we increased the insertion of one of the BK7 prisms so as to add 1 mm of glass to the total beam path. The automated optimization routine was run again and the FROG trace compared with that obtained without the extra glass. The results were identical within error, proving that the optimal solution was well within the pulse shaping limits of the apparatus. We note that a slight degree of chromatic separation was observed when the full voltage was applied to all pixels. None the less the latter test demonstrated that this was not a factor in determining the pulse fitness or the optimal GDD.

As a complementary measure of the optimal pulse performance in minimizing population transfer, and as a guide for simulations of the excitation dynamics we measured the degree

of saturation obtained at the various fluences studied. The fluence dependent degree of saturation, $S(F)$, was defined as

$$S(F) = V_f(F)/V_f(0)$$

where $V_f(F)$ is the fluorescence signal obtained by the optimized pulses at fluence F, and $V_f(0)$ is that obtained for a negligible pump fluence. The latter was determined by reducing the pump energy by a factor of 10, grounding all mirror channels, and displacing the cell to a point where further displacement (increase in excitation beam diameter) did not effect the emission signal. Ten times that signal was used to approximate $V_f(0)$. Thus, while $V_f(0)$ is an asymptotic limiting value which is in practice not directly measurable, by reducing the fluence sufficiently we believe that we have a close approximation of its value. The results for $S(F)$ are depicted in Figure 2. As shown in the inset $S(F)$ is a nearly linear function of $\log(F)$ over the fluence range studied.

The multichannel experiment was performed on LDS-750 in acetonitrile in the same sample cell. A similar amplified titanium sapphire laser was operated at 190 Hz, with most of the output pumping a TOPAS optical parametric amplifier (Quantronix). The doubled output from the TOPAS at ~600 nm was compressed to ~20 fs with prisms, and used as a pump source in a multichannel double spectrometer system which has been described in detail in the literature.[32] The supercontinuum probe pulses which were split to produce a probe spectrum in one spectrograph, and a reference spectrum in the other, were generated with a fraction of the 790 nm fundamental in a 1 mm sapphire plate. The transient transmission spectra following 600 nm excitation of a 0.4 OD LDS750 solution in acetonitrile, in the range from 500 to 900 nm, were recorded at pump−probe delay intervals of 3 fs. The transient spectra were later corrected for the probe group delay dispersion.

Results and Discussion

Results of optimization runs in acetonitrile are presented in Figure 4 where a series of FROG traces of the optimal pulses at various excitation fluences are shown. In the last panel, a plot of the GDD curves obtained from the contour maps above are presented for comparison. These curves are obtained by performing a Gaussian fit to sections of the FROG data at each wavelength, and taking the origin of each as the group delay for that specific color. The similarity of the GDD at the different fluences is obvious both from the FROG traces themselves, and from the GDD curves below. The curves are nearly identical over the range from 550 to 670 where the pulse intensity is large, with differences increasing beyond this range, presumably due to reduced evolutionary pressures on lower intensity frequency components.

The optimal GDD for minimizing LDS750 fluorescence in acetonitrile has the following functional form. At frequencies below 580 nm the group delay is constant, indicating that this portion of the NOPA spectrum comprises a nearly transform limited pulse. At higher wavelengths the spectral components arrive at later and later delays. The chirp rate is nearly constant at first with a GDD of -140 fs^2/rad up to $\lambda \sim 660$ nm, slowing even further beyond that wavelength. As demonstrated by the comparison of the FROG contour plots in Figure 5, this general structure is conserved within error for the case of ethanol solutions as well. Before comparing the results for acetonitrile with those in alcohol, the Kerr data were averaged for optimization runs at a number of intermediate fluences for both solvents in order to reduce any spurious noise from the data.

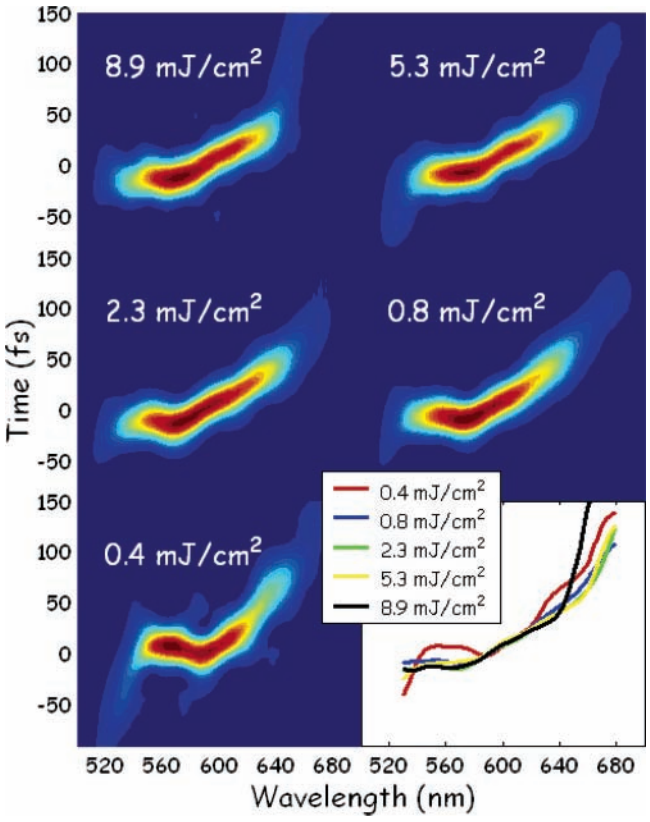

Figure 4. FROG data of pulses which minimize fluorescence in acetonitrile solutions of LDS750 at five different fluences. The last panel is the GDD of the pulses obtained from the contour plots above. See text for details.

We note that in cases where multiple distinct solutions arise from the optimization process, averaging makes no sense. Here we average FROG traces which have already been demonstrated to be virtually the same just to eliminate noise due the measurement itself. The results show that while the GDD curves in both solvents are similar, with close to zero GDD below 580 nm, the chirp rate is somewhat lower in ethanol, and the further falling off is slightly earlier in that solvent. These differences are however on par with the variations observed in a single solvent from run to run, showing that the optimal pulse shape is almost invariant to this change of solvent.

To assess the strategy by which minimal population transfer is achieved in these experiments, we compare the optimal GDD with multichannel transient transmission data measured in acetonitrile, as depicted in Figure 6. The upper panel shows the linear absorption and the time integrated fluorescence spectra of LDS750 in acetonitrile, along with the intensity spectrum of our NOPA pulses. In addition we include a stimulated emission spectrum which is synthesized from that of the absorption curve included in this graph.[33] It represents the cross section which would exist for stimulating emission from the initially excited state after vibrational dephasing and population relaxation, assuming isomerization on this potential does not take place, and serves as an aid in analyzing our results.

The lower panel displays a contour plot of the transient spectral variations induced by 600 nm photoexcitation of LDS750 in acetonitrile as a function of pump−probe delay in the range from 500 to 900 nm. Increased transmission is depicted in shades of red and brown, with excess absorption in shades of blue (see ΔOD scale on the color bar). As described by Ernsting and co-workers, excitation gives rise to an instantaneous excited state absorption band to the blue of that of the

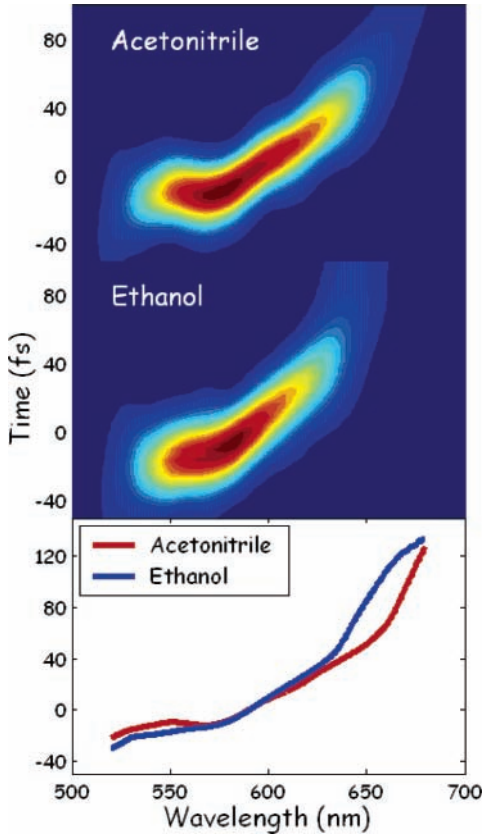

Figure 5. Averaged polarization gate FROG data of NOPA pulses which minimize fluorescence from LDS750 solutions in acetonitrile (upper panel) and ethanol (middle panel). On the lower panel, the GDD of the pulses above is plotted for comparison.

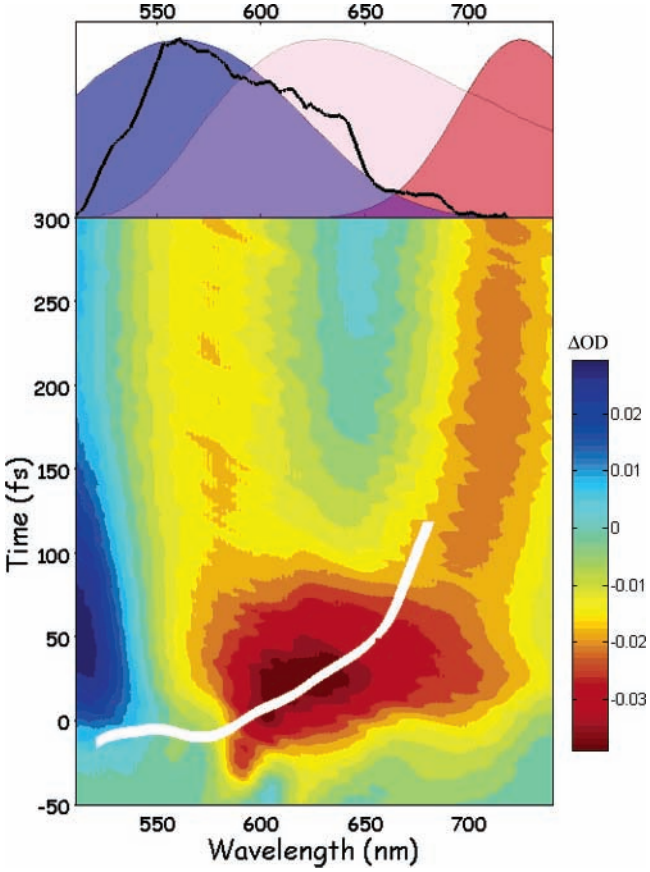

Figure 6. Absorption (blue) and fluorescence (red) spectra of LDS750 in acetonitrile are plotted in the upper panel. A calculated stimulated emission spectrum for a relaxed locally excited state is also depicted in light red. In the lower panel a contour plot of multichannel transient absorption spectra of LDS750 in acetonitrile is plotted as a function of pump−probe delay time. The white line is the GDD of the optimal NOPA pulse which was obtained from the polarization gate FROG in Figure 5, as a function of gate delay. See text for details.

ground state. Emission and ground state bleach overlap at early delay times to produce a broad excess transmission feature which gradually separates into two distinct bands due to ground-state relaxation, and excited-state isomerization.[22] Juxtaposed on this contour plot is the averaged optimal GDD obtained from the FROG scans in acetonitrile and depicted in Figure 5. The transform limited "blue" edge of the GDD curve has been shifted in time to coincide with time zero of the multichannel data. Even on a phenomenological level, the comparison of the GDD and multichannel data shows that the spectral components above 580 closely follow the Stokes shifting of the emission band, demonstrating the utility of this spectroscopic tool in covering ultrafast spectral evolution in the excited sample.

In view of the compiled data in Figure 6, our understanding of how these pulses realize maximal transparency is as follows: The blue transform limited portion builds up an impulsive "initiation" pulse, which serves to launch a focused wave packet on the excited surface. Characterization of this interaction as "impulsive" is somewhat loose, as it mainly pertains to lower frequency nuclear motions associated with the rapid isomerization, and potentially also to solvation coordinates. Following the blue "initiation" interaction, the remainder of the NOPA field comprises a "tracking" chirped red tail which follows the evolving excited population in frequency and in time, and efficiently stimulates emission as the excited state dynamics are underway. This GDD thus produces an ideal single pulse concerted pump−dump sequence which optimally obtains the control objective of inducing transparency and minimizing the ultimate population of the excited state.

The subdivision of the pulse spectrum into initiating and following portions requires further comment. The former must involve the blue edge of the spectrum for obvious reasons, but also be broad enough in frequency to prepare a localized wave packet on the excited surface which can be efficiently followed. It also stands to reason that components of the pulse which are dominated spectrally by ground state absorption will contribute to the initializing interaction. This point is complicated since even without isomerization, excited state vibrational excess energy and coherence will both influence its spectral response. Short of a full fledged simulation, we can only surmise that the latter consideration is a determining factor here. As a guide in this respect we have plotted the simulated spectrum in the upper panel of Figure 6, which shows that a relaxed excited state prior to isomerization (a state which is not realized at any stage of our experiment) would in fact have a stimulated emission spectrum which dominates the absorption at wavelengths above 600 nm. It is therefore plausible that both factors determine the division of pulse spectral components as described above. We note however that the slight red shifting in the absorption spectrum of LDS750 in ethanol does not lead to an observable shift in the pulse spectrum division between initiation and emission following.

While this interpretation makes mechanistic sense, it is challenging to rationalize why the change of solvent and the variation of pulse fluence by factors of more than 10 do little to alter the optimal pulse shape for obtaining this goal. We will start by discussing the absence of solvent effects on the optimal fields. LDS750 is known to exhibit imbalance in the spectral

widths and solvent shifts observed in its absorption and steady-state emission bands.[22,23] The absorption is extensively broadened and blue shifts markedly when dissolved in polar solvents. In contrast, the emission is narrower, shows weak vibronic structure, and varies only slightly with change in solvent polarity. The dipoles for these two transitions differ by more than a factor of 2. Accordingly, only a significant rearrangement or isomerization in the excited state could render these two transitions, which would otherwise be mirror images of each other, to differ in this fashion.

A number of experimental studies using broadband pump−probe, resonance Raman, and photon echo techniques have been conducted to obtain information concerning the dynamics of structural changes which underlie the linear spectroscopy of LDS750.[22−24] Disregarding mild discrepancies in their findings, the results show that due to the plethora of active vibrational modes and existence of reactive isomerization routes opened up by photoexcitation, much of the dynamics in the excited state are dictated by intramolecular motions, including the dephasing of the absorption transition dipole, and the dynamic Stokes shifting of fluorescence. None the less, solvent effects were observed on the durations of all of these time scales. While deuteration of methonol solvent molecules did not effect the electronic dephasing times as measured by RR intensities, photon echo experiments[23] showed some differences in the time scale of this process when the solvent was changed to acetonitrile. The excited-state isomerization which takes place in ∼200 fs and contributes dominantly to the fluorescence red shift, was shown to be more than two times slower when the solvent is changed from acetonitrile to chloroform.

Our choice of ethanol and acetonitrile was aimed at comparing solvents which have similar overall Stokes shifts and absorption spectra, but which differ markedly in the amplitudes of inertial and relaxational solvation.[34] Inertial solvation was assumed to be most relevant to minimizing population transfer in view of the optimal amount of linear chirp obtained by the Shank group which resulted in a total excitation pulse duration of less than 100 fs.[11] Without detailed transient spectral data for the alcohol solutions to compare with those in acetonitrile, it is hard to comment on expected changes in the pulse shapes which minimize fluorescence in the two solvents. We conclude that the specific change in solvent conducted here has a negligible effect on the dynamic Stokes shifting of impulsively excited LDS750 molecules, and also that moderate changes in the time scale of electronic dephasing which were discovered in the three pulse photon echoes have little effect on the process at hand. Experiments aimed at verifying this by multichannel spectral probing in ethanol solutions as well are underway in our laboratory. Experiments with a broader range of solvents will probably allow a fuller assessment of the role played by solvation in obtaining minimal population transfer in this particular dye.

The absence of intensity effects on the optimal excitation field seems much harder to understand. While this is in accord with the findings of Cerullo et al. that the optimal *linear* chirp for fluorescence minimization was insensitive to fluence, we would expect such a dependence for automated shaping schemes for a number of reasons. First, in their earlier study, Ernsting and co-workers discovered that by varying the excitation fluence of 40 fs excitation pulses at 530 nm one can go from predomenant population of the first excited singlet, to almost exclusive excitation of higher electronic states via stepwise multiphoton absorption (MPA).[22] The fluence range reported in that study lies within that experimented with here. Accordingly we would expect that an increase in our pulse fluence would lead to enhanced involvement of MPA as well. Since the higher excited states led to delayed population of the fully relaxed fluorescent state, such an involvement would necessarily have an effect on the overall emission efficiency, and require alterations in the optimal excitation GDD for minimizing fluorescence—contrary to our finding.

Second, accepting the intrapulse pump−dump mechanism as the correct explanation of the optimal GDD, achieving a 2π Rabi cycle with transform limited pulses might have advantages over the chirped tracking strategy which is envisioned here at high pulse fluences. Such an opportunity would not exist at lower fluences due to insufficient "pulse area". Finally, despite the determining factors discussed above for the division of pulse frequency components, such large changes in fluence could alter the balance between them and vary the breaking point between promotion and following. Factoring in the influences of rapid electronic dephasing in the liquid environment, significant variations in optimization strategies and changes of optimal pulse structure with the variation of fluence would be plausible or even expected. This is true even when we consider the continuous radial distribution of fluences characteristic of a Gaussian laser beam, and the random orientation of the dye molecules. The range of fluences experimented with is so extensive that even the averaging effects presented by the near TEM00 intensity distribution would not average out if a significantly new optimization strategy were possible at the higher end. Despite this, we have observed no significant changes. Theoretical simulations to understand this result are underway in collaboration with R. Kosloff and co-workers.

One must consider how the limitations of our pulse shaper affect the solutions derived from it. Our criteria for convergence of the GA's random search were the incremental improvements in fitness obtained for successive generations, and a comparison of the FROG traces of the resulting pulse shapes for repeated optimization runs. The consistent equivalence of the optimal pulse performance and of its GDD from run to run, along with the absence of voltage saturation on any of the mirror channels, indicates that a close semblance of the true optimal field which is achievable by the shaper was obtained. While this field may be limited by the shaper capabilities, the repeatability of the optimal pulse suggests that none of the modulation components is redundant, as observed in some recent control experiments using other shaping methods.[35] Accordingly, it is important to consider the space of possible pulse shapes within which the search is conducted. The inability of the DM to modulate intensities is not a limitation here since our aim was to alter phase and not amplitude. However, even in terms of phase, the DM is the least versatile automated phase modulation method, with its high throughput and rapid updating being its main advantages. The lack of true pixilation of phase modulation which prohibits the DM from "wrapping phase" seriously curtails the range of pulse shapes obtainable to nonlinear continuous chirps within a limited range of total pulse duration. In our case, the limiting total duration is demonstrated in Figure 3 to be ∼315 fs fwhm for predominantly negatively chirped pulses.

It is possible that a superior pulse shape exists, which is based on longer total pulse duration or more intricate phase compositions, but is unattainable by the DM based shaper. One could envision a pulse GDD, which might be generated by other shaping methods,[36,37] which follows periodical spectral modulation due to vibronic coherences in either electronic state etc.[38,39] Experiments aimed at investigating this point with alternative

shaping methods are under way in our laboratory. In the present case the chances that such limitations of the shaper have obscured such a possibility are slim, since our pulse spectrum overlaps negligibly with that of the steady state fluorescence, and vibronic coherences do not heavily modulate impulsive pump−probe data of LDS750 as in other dye solutions.[23] Our results and the discussion above do stress that broad spectral coverage is prerequisite to gaining meaningful automated quantum control of the sort we have attempted.

Finally, we discuss the merit of the above experimental approach to photochemically important molecular systems. Clearly, the main objective of the current experiments was not the investigation of excited state dynamics in LDS750 per se, but rather assessing the above experimental approach as a general spectroscopic tool for following such dynamics. Even if one accepts the potential of computer controlled self-induced transparency as a useful addition to existing spectroscopic methods for following ultrafast photoinduced dynamics, in many photochemically interesting molecules fluorescence is quenched by reaction. Without spontaneous emission to gauge population transfer, one must look for alternative ways of measuring the energy balance between the field and the material system. In their original paper, Cerullo et al. measured the change in the transmitted excitation pulse spectrum with positive and negative linear chirp. In the latter case, an obvious shift of the pulse energy to the red was observed as one would expect for a pump−dump sequence with simultaneous Stokes shifting. One could use the pulse energy and spectrum to follow the said energy balance, but it would require precise calibration of the detection setup.[39] Furthermore, it would also require dealing with samples which are not optically thin, leading to an inherent distribution of intensities even along the propagation direction, and enhanced propagation effects. Even then, maximizing photon transmission, or minimizing fluorescence, is far from the same thing when the possibility for MPA exists as it does even for the case at hand. The feasibility of using transmitted photon counting as an alternative measure of excitation probability will best be tested for a case where it can be compared with that of spontaneous emission, as in the case of LDS750 or other fluorescent molecules. This approach is also being pursued in our laboratory, to test the applicability of this novel tool to nonfluorescent reactive systems.

Conclusions

An adaptive pulse shaping setup based on a deformable mirror, and directed by a genetic algorithm, has been used to nonlinearly chirp broadband NOPA pulses so as to minimize fluorescence from LDS750 in acetonitrile and ethanol. The resulting optimal pulse shape consisted of two parts. The high frequency portion of the NOPA pulse spectrum below 580 nm comprised a nearly transform limited initiation pulse which is interpreted to prepare a localized wave packet on the excited electronic state. The remainder of the excitation field was negatively chirped in a fashion which was shown to follow the dynamic Stokes shifting of the excited-state emission. This was confirmed by comparing the resulting GDD of the optimal pulses with impulsive multichannel pump−probe data in acetonitrile solutions of the same dye. Changing the solvent from acetonitrile to ethanol, or increasing the pulse fluence by more than an order of magnitude, had a negligible effect on the optimal chirp for minimizing population transfer in LDS750. We conclude from the weak solvent dependence that rapid spectral evolution in emission of LDS750 is not strongly altered by the shift between these solvents. This is in accord with earlier studies showing that much of the rapid Stokes shifting in LDS750 reflects intramolecular rather than intermolecular dynamics. The absence of fluence effects on the optimal pulse shape obtained will be the subject of further theoretical and experimental study. The results reported demonstrate the utility of this experimental approach for recording rapid spectral evolution of nascent excited states in fluorescent chromophores.

Acknowledgment. We wish to thank Professors R. A. Bartels, M. M. Murnane, and H. C. Kapteyn, for sharing the genetic algorithm code, and Prof. N Ernsting and Dr. L. Lusters, for assisting in the setup and operation of the multichannel apparatus. We thank Prof. G. Cerullo and C. Manzoni, for NOPA advice, and Prof. D. Huppert, for a dye sample. This research was funded by the German Israeli Cooperation in Ultrafast Laser Technologies (GILCULT). The Farkas research center is supported by the Minerva Gesellschaft, GmbH, Munich, Germany.

References and Notes

(1) Brixner, T.; Gerber, G. *ChemPhysChem* **2003**, *4*, 418.
(2) Goswami, D. *Phys. Rep.—Rev. Sect. Phys. Lett.* **2003**, *374*, 385.
(3) Rice, S. A.; Zhao, M. *Optical Control of Molecular Dynamics*; Wiley: New York, 2000.
(4) Levis, R. J.; Rabitz, H. A. *J. Phys. Chem. A* **2002**, *106*, 6427.
(5) Kawashima, H.; Wefers, M. M.; Nelson, K. A. *Annu. Rev. Phys. Chem.* **1995**, *46*, 627.
(6) Shi, S.; Woody, A.; Rabitz, H. *J. Chem. Phys.* **1988**, *88*, 6870.
(7) Chelkowski, S.; Bandrauk, A. D.; Corkum, P. B. *Phys. Rev. Lett.* **1990**, *65*, 2355.
(8) Krause, J. L.; Whitnell, R. M.; Wilson, K. R.; Yan, Y.; Mukamel, S. *J. Chem. Phys.* **1993**, *99*, 6562.
(9) Melinger, J. S.; Gandhi, S. F. L.; Hariharan, A.; Goswami, D.; Warren, W. S. *J. Chem. Phys.* **1994**, *101*, 6439.
(10) Ruhman, S.; Kosloff, R. *J. Opt. Sot. Am. B* **1990**, *7*, 1748.
(11) Cerullo, G.; Bardeen, C. J.; Wang, Q.; Shank, C. V. *Chem. Phys. Lett.* **1996**, *262*, 362.
(12) Barbara, P. F.; Jarzeba, W. *Adv. Photochem.* **1990**, *15*, 1.
(13) Bagchi, B.; Chandra, A. *Adv. Chem. Phys.* **1991**, *80*, 1.
(14) Maroncelli, M. *J. Mol. Liq.* **1993**, *57*, 1.
(15) Neria, E.; Nitzan, A. *J. Chem. Phys.* **1994**, *100*, 3855.
(16) Cho, M.; Fleming, G. R. *Annu. Rev. Phys. Chem.* **1996**, *47*, 109.
(17) Glasbeek, M.; Zhang, H. *Chem. Rev.* **2004**, *104*, 1929;.
(18) Ingrosso, F.; Ladanyi, B. M.; Mennucci, B.; Elola, M. D.; Tomasi, J. *J. Phys. Chem. B* **2005**, *109*, 3553.
(19) Bardeen, C. J.; Wang, Q.; Shank, C. V. *Phys. Rev. Lett.* **1995**, *75*, 3410; *J. Phys. Chem. A* **1998**, *102*, 2759.
(20) Lanzani, G.; Zavelani-Rossi, M.; Cerullo, G.; Comoretto, D.; Dellepiane, G. *Phys. Rev. B* **2004**, *69*, 134302.
(21) Bardeen, C. J.; Yakovlev, V. V.; Wilson, K. R.; Carpenter, S. D.; Weber, P. M.; Warren, W. S. *Chem. Phys. Lett.* **1997**, *280*, 151.
(22) Kovalenko, S. A.; Ernsting, N. P.; Ruthmann, J. *J. Chem. Phys.* **1997**, *106*, 3504.
(23) Bardeen, C. J.; Rosenthal, S. J.; Shank, C. V. *J. Phys. Chem. A* **1999**, *103*, 10506.
(24) Knorr, F. J.; Wall, M. H.; McHale, J. L. *J. Phys. Chem. A* **2000**, *104*, 9494.
(25) Rosenthal, S. J.; Jimenez, R.; Fleming, G. R.; Kumar, P. V.; Maroncelli, M. *J. Mol. Liq.* **1994**, *60*, 25.; Bingemann, D.; Ernsting, N. P. *J. Chem. Phys.* **1995**, *102*, 2691.
(26) Gershgoren, E.; Vala, J.; Kosloff, R.; Ruhman, S. *J. Phys. Chem. A* **2001**, *105*, 5081.
(27) Cerullo, G.; De Silvestri, S. *Rev. Sci. Instrum.* **2003**, *74*, 1.
(28) Zeek, E.; Maginnis, K.; Backus, S.; Russek, U.; Murnane, M.; Mourou, G. R.; Kapteyn, H.; Vdovin, G. *Opt. Lett.* **1999**, *24*, 493.
(29) Baum, P.; Lochbrunner, S.; Gallmann, L.; Steinmeyer, G.; Keller, U.; Riedle, E. *Appl. Phys. B: Laser Opt.* **2002**, *74 [Suppl.]*, S219.
(30) Zeek, E.; Bartels, R.; Murnane, M. M.; Kapteyn, H. C.; Backus, S.; Vdovin, G. *Opt. Lett.* **2000**, *25*, 587. Bartels, R. A. Ph.D. Thesis, University of Michigan, 2002.
(31) Trebino, R.; DeLong, K. W.; Fittinghoff, D. N.; Sweetser, J. N.; Krumbugel, M. A.; Richman, B. A.; Kane, D. J. *Rev. Sci. Instrum.* **1997**, *68*, 3277.

(32) Ernsting, N. P.; Kovalenko, S. A.; Senyushkina, T.; Saam, J.; Farztdinov, V. *J. Phys. Chem. A* **2001**, *105*, 3443.

(33) The stimulated emission curve is calculated from the absorption spectrum of LDS750 in acetonitrile, using the simplified vibronic analysis presented by Kovalenko et al. in ref 22.

(34) Horng, M. L.; Gardecki, J.; Papazyan, A.; Maroncelli, M. *J. Phys. Chem.* **1995**, *99*, 17311.

(35) Langhojer, F.; Cardoza, D.; Baertschy, M.; Weinacht, T. *J. Chem. Phys.* **2005**, *122*, 014102.

(36) Wefers, M.; Nelson, K. *Opt. Lett.* **1993**, *18*, 2033.

(37) Hillegas, C. W.; Tull, J. X.; Goswami, D.; Stricland, D.; Warren, W. S. *Opt. Lett.* **1994**, *19*, 737.

(38) Hornung, T.; Meier, R.; Motzkus, M. *Chem. Phys. Lett.* **2000**, *326*, 445. Lindinger, A.; Lupulescu, C.; Plewicki, M.; Vetter, F.; Merli, A.; Weber, S. M.; Woste, L. *Phys. Rev. Lett.* **2004**, *93* (3), 033001/1.

(39) After submission of this manuscript we become aware of a low intensity coherent control experiment: Prokhorenko, V. I.; Nagy, A. M.; Miller, R. J. D. *J. Chem. Phys.* **2005**, *122*, 184502, which does in fact demonstrate the following of coherent vibrational motion in acousto-optically shaped fields which optimize population transfer in dye solutions.